

## Design and Application of a Zircon Advanced Refractory Ceramic

R.C Garvie, J.Drennan, M.F. Goss, S. Marshall, and C.Urbani

CSIRO, Division of Materials Science and Technology  
Clayton, Victoria 3168, Australia

## Abstract

A strong, thermal shock resistant zircon advanced refractory ceramic (ZS10) was designed by dispersing 10 weight percent monoclinic zirconia polycrystalline (MZP) particles in a dense matrix. The dispersion of MZP induced thermal shock resistance via a new toughening mechanism unrelated to transformation toughening. Laboratory tests showed that ZS10 had superior corrosion resistance in molten E-glass compared to conventional zircon refractories and was equivalent to them in thermal shock resistance. Accordingly, a field test was conducted on a ZS10 bushing block. The fabrication and performance of the block are described.

## Introduction

Traditional refractories cannot be simultaneously dense and thermal shock resistant.<sup>1</sup> The reason is that the pores in these materials induce stable crack propagation by virtue of the fact that they are stress concentrators.<sup>2</sup> As such they generate a network of microcracks in regions of material subject to thermal shock; this is a recognised toughening mechanism. Unfortunately, using a dispersion of pores as a toughening mechanism greatly weakens the material and reduces its resistance to erosion and corrosion; in this sense a refractory is a badly degraded ceramic.

The traditional trade off in the properties of refractories can be overcome by dispersing solid particles in the matrix which can perform the same function as pores. Such particles should display highly localised self-stresses which can be transmitted to the surrounding matrix. One material of choice for this purpose is monoclinic zirconia whose transformational strains have long been used to toughen a variety of refractories and ceramics. However, the chief difficulty with a toughening mechanism based on the tetragonal/zirconia phase transformation is that it is strongly and inversely dependent on temperature.<sup>3</sup>

A better choice is monoclinic polycrystalline zirconia particles. The reason is that these particles are self-stressed due to their severe anisotropy of thermal expansion; moreover, the intrinsic thermal stresses are amplified by virtue of the polycrystalline morphology of the particles.<sup>4-5</sup> A considerable advantage of a system designed in this way is

that the toughening mechanism functions at least up until the monoclinic to tetragonal transformation temperature at about 1200°C. However, tetragonal zirconia itself has an appreciable thermal expansion anisotropy so that some toughening can be expected from this source until some temperature such that intrinsic stress relieving mechanisms are activated in the matrix. In this condition, the matrix itself would display intrinsic thermal shock resistance.

The purpose of this work is to describe the preparation, characterisation and application in the glass industry of an advanced zircon refractory ceramic toughened with a dispersion of MZP.

### Experimental

The MZP was comprised of aggregates with an overall size of 13µm. An aggregate, itself, consisted of microcrystals about 1-2µm in diameter which were strongly bonded together. This fine structure is stable; no change was observed after it was heated at 1600°C/1hr. A screening test revealed that the optimum concentration of MZP was 10 wt %; samples of this composition are designated ZS10.

Laboratory samples were prepared by making a slurry of MZP and zircon powder<sup>^</sup> in isopropyl alcohol together with a fugitive wax binder; the latter amounted to 4 wt % of the dry solids. The powder had a mean particle size of 1.5µm. After mixing in a Glen Creston mill with plastic balls for 15 minutes, the slurry was evaporated to dryness. Then the powder batch was granulated successively through 20- and 50- mesh screens. After being formed by die pressing, test billets were isostatically pressed at 210MPa. The billets then were fired at 1600°C/1hr to attain a density of about 92% of the theoretical value. The billets were machined by diamond grinding to a standard size of about 3x3x40mm.

Similarly, billets of pure zircon (ZS) and also zircon containing a dispersion of 10 wt. % baddelyite particles<sup>\*\*</sup> (ZB10) were prepared for purposes of comparison. The single crystal baddelyite particles were milled to obtain a particle size distribution close to that of the MZP aggregates. A second set of larger billets of ZS and ZS10, 25x25x75mm, was prepared in the same way except that they were not diamond ground.

The thermal shock behaviour of ZS, ZB10 and ZS10 was determined by quenching the small test billets, which had been progressively heated to various temperatures, into water at

---

<sup>^</sup>S-grade, Magnesium Elektron Ltd., Manchester, U.K.

<sup>\*\*</sup>Opacifine 5, Curumbin Minerals Ltd., Curumbin, Qld., Australia.

<sup>\*\*</sup>400-K, Mandoval Ltd., Lightwater, Surrey, U.K.

room temperature. Also the thermal shock fatigue behaviour of ZS and ZS10 was determined using an industry standard test.<sup>6</sup> One fatigue cycle consisted of inserting a cold billet into a furnace for 15 minutes which had been preheated to 1400°C and then allowing it to cool outside the furnace for 15 minutes. A sample failed when its weight loss due to spalling amounted to 5%. The score achieved by a billet was the number of cycles attained at failure.

ACI Ltd. performed corrosion tests on ZS10 in which a cylindrical sample, 25x150mm, was immersed in molten E-glass at 1330°C and rotated for 235 hours. A photograph of the test facility is shown in Figure 4. The figure of merit used to assess the rate of corrosion was the percent decrease in the diameter of the sample measured at a point  $\frac{1}{2}$  the distance between the glass line and the immersed end of the sample. Other commercial zircon refractories were tested simultaneously for purposes of comparison. The results are summarised in Figure 6.

On the basis of combined thermal shock and corrosion data for ZS10, the ACI Fibreglass, Dandenong, Victoria agreed to install a prototype bushing block made of ZS10 in their production line. A scaled up version of the laboratory process was used to make the block as follows. An aqueous slurry containing about 71 % solids and 2 wt % (solids basis) of an organic binder was spray dried. The powder batch was then isostatically pressed at 200MPa to form an oversized rectangular block weighing about 40 kgm. The block was fired at 15°C/hr until 500°C and then at 50°C/hr from 500°C to 1400°C; the block was held at this temperature for 2hr. Then heating was resumed at the same rate to 1600°C where it was held again for 2 hr. At the end of the soak period the block was furnace cooled to room temperature. Finally it was diamond ground to tolerance and the central channel formed by trepanning with a diamond tool.

A 'post-mortem' examination of the ZS10 block was performed using transmission optical microscopy (TEM), optical microscopy and x-ray energy dispersion analysis.

## Results and Discussion

### 1. Laboratory tests

The thermal shock behaviour of the three zircon based materials is shown in Figure 1 which is a plot of the strength retained in damaged billets (MOR) as a function of the quenching temperature difference ( $T^{\circ}\text{C}$ ). The pure matrix phase, ZS, showed behaviour typical of a dense brittle material (Figure 1a); i.e., after an initial plateau a critical quenching temperature difference (330°C) is reached which activates preexisting surface flaws resulting in a catastrophic decrease in strength (unstable crack propagation) to a second plateau. At the second plateau there is a second critical quenching temperature difference at about 660°C which heralds the onset of stable crack propagation; i.e., with

increasing severity of thermal shock there is only a gentle decline in retained strength. Stable crack propagation is synonymous with thermal shock resistance.

The thermal shock resistance of the ZB10 billets (Figure 1b) is improved by the dispersion of baddelyite particles in that the critical quenching temperature difference for the onset of unstable crack propagation is increased to about 360°C and the degradation of the strength from to unstable crack propagation is reduced. The modest increase in toughness could be due to crack bowing/ deflection by the single crystal zirconia particles.

The dispersion of MZP has considerably enhanced the thermal shock resistance of ZS10 because it displays only stable crack propagation (Figure 1c). There must be an additional contribution to the toughening increment in addition to crack bowing/deflection.

One plausible mechanism is based on the severe thermal expansion anisotropy of monoclinic zirconia. During cooling of a sample of ZS10 to room temperature after sintering, considerable thermal stresses would be generated in the aggregates. Moreover these stresses would be amplified by up to a factor of 3 because of the polycrystalline morphology of the particles. These stresses would be transmitted efficiently to the matrix because the dilatational strain during the tetragonal to monoclinic transformation guarantees intimate contact between particle and host at their interface. In any region of ZS10 subject to thermal shock, stresses so generated would be superimposed onto the preexisting stresses arising from the anisotropy with the possibility of nucleating microcracks.<sup>4-5</sup> In this way, the dispersed MZP particles behave like pores with the considerable advantage of preserving much of the original strength of the material.

The improvement in mechanical properties possible with a dispersion of MZP as a toughening agent rather than pores is demonstrated by the data in table 1. The strength and Young's modulus of ZS10 are improved by several hundred percent compared to the values for a commercial zircon refractory.<sup>7</sup> The reason is that the porosity of the former is 8% whilst that of the latter is more than 20%. Yet the thermal shock resistance parameter,  $R_{st}$  ( $=\tau_{NPF}/\tau_{NBT}$ ) is about the same for both materials.

Direct evidence of a toughening mechanism operating in ZS10 is shown by Figure 2 which features optical micrographs of thermally shocked ZS and ZS10. The former material displays long straight through cracks characteristic of unstable crack propagation. The latter shows strong crack/particle interaction with many instances of crack branching and crack arrest, indicative of stable crack propagation.

Figure 3 shows the results of the industry standard thermal fatigue test applied to ZS and ZS10. The pure matrix material, ZS, shattered upon its first insertion in the

furnace thereby acquiring a score of  $\frac{1}{2}$ ; ZS10 showed no weight loss by spalling after 20 fatigue cycles and received a score of 20. Experience with this test indicates that little further damage occurs after 20 cycles so that there is no point in continuing the test beyond this point. Similar thermal fatigue data for various commercial zircon refractories are summarised in Figure 6 and is discussed below.

The test rig used to obtain estimates of the relative rates of corrosion of the zircon refractories in E-glass is shown in Figure 4. Figure 5 is a photograph of the ZS10 and zircon samples after the corrosion test in E-glass. The results are summarised in Figure 6 together with the results of the thermal fatigue test; the corrosion rate and the thermal shock fatigue data are plotted together as a function of porosity. The corrosion rate increases almost exponentially as a function of the porosity of the various refractories. A similar dependency has been observed for slag corrosion tests.<sup>1</sup> ZS10, as the densest material, had the lowest rate of corrosion. The datum point labelled 'zircon 20' refers to the present industry standard material for the bushing block application. The thermal shock behaviour of the commercial refractories follows the expected pattern which is opposite to the trend observed for the corrosion data; the porous materials have a high value of the figure-of-merit for thermal shock resistance which decreases sharply with increasing density. The thermal shock data for the dense ZS10 is anomalous in that it is equivalent to the porous materials, due to its toughening mechanism.

## 2. Field Test

The results of the laboratory thermal shock and corrosion tests indicated that ZS10 could be a candidate material for industrial applications. A suitable application is the bushing block used in the fibre glass industry to meter molten E-glass to the Pt/Rh bushing which forms the fibres. A schematic of the fibre glass process is shown in Figure 7.

The bushing is usually replaced annually because the forming holes have become too enlarged. The replacement is straight forward requiring only a short down time. The bushing block is replaced at the same time but requires a down time of several hours and several personnel so that it represents a serious loss of production. There would be a considerable increase in productivity if the blocks only needed replacement biannually instead of annually. This was the motivation for testing the ZS10 block in the field.

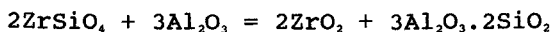
Two blocks were fabricated with the assistance of local industries (Figure 8). One block was installed in the production line of a local fibre glass producer (Figure 9) on 4 June 1987. After fixing the block and bushing in place the temperature of the ensemble was increased to the operating value according to the following schedule; from an initial value of around 430-480°C, the rate was 6.5°C/min. to 660°C

with a soaking time of 30 minutes; then heating was resumed at the same rate to 980°C for another soak of 30 minutes. Heating is done electrically by passing a current through the bushing. The unit operated until 6 May, 1988 after metering 386 tonnes of glass; it was shut down for technical reasons related to the melter. The performance of the block was marred by enhanced stoning which was observed during all stages of the test; the reason for this will be discussed below. The shut down involves circulating cooling water through the bushing. After the bushing is removed the block is hosed down with cold water until it can be removed manually using jack hammers, etc.

Figure 10 is a photograph of the used ZS10 block which shows that it has reasonable mechanical integrity. Probably the integrity could be improved further by encasing the block in a steel band around its circumference.

Unfortunately the chemical integrity of the ZS10 block was compromised by the micronising process which used alumina grinding media. The resulting alumina contamination (table 2) allowed the formation of a glassy phase in the grain boundaries as shown by the TEM micrograph in Figure 11. Further evidence for the formation of a high alumina grain boundary phase was obtained by x-ray energy dispersion analysis of a grain boundary and also pristine bulk material (Figure 12).

It the presence of alumina was known at the beginning of the project but it was thought to be harmless because it ought to form isolated mullite grains according to the well known reaction;



The presence of a glassy grain boundary phase allowed the easy penetration of E-glass into the ZS10 block. The E-glass dissolved the dispersed zirconia phase preferentially which probably contributed to the enhanced stoning noted in the later stages of the test. The optical micrograph in Figure 13 illustrates the penetration and preferred dissolution phenomena; glass has entered a thermal shock crack and penetrated the refractory adjacent to the crack boundaries. Unfortunately, the laboratory corrosion test did not reveal the stoning problem. With hindsight, the zircon powder should have been micronised with steel grinding media and then washed with acid.

## Conclusions

It has been shown that a zircon/zirconia alloy, ZS10, a member of new category of dense, advanced refractory ceramics can be used in an industrial application involving severe thermal shock.

The performance of the block warranted further tests although chemical contamination of the zircon used in the bushing block application prevented a definitive conclusion as to whether use of the new material would enhance productivity of fibre glass production.

## Acknowledgements

We thank Mr. Rodd Judd, Laboratory Services Glass Packaging Division, ACI Ltd. for performing the glass corrosion tests and Dr. Paul Flavel, Technical Manager, Reinforcements, ACI Fibreglass for supervising the field test. Also we are grateful to Magnesium Elektron Ltd. for partial financial support of this work.

## References

1. W.S. Trettner, "Refractories Technology", Bull. Am. Ceram. Soc., 58, 715-18 (1979).
2. R.D. Smith, H.U. Anderson and R.E. Moore, "Influence of Induced Porosity on the Thermal Shock Characteristics of  $Al_2O_3$ ", *ibid*, 55, 979-82 (1976).
3. M.V. Swain, R.H.J. Hannink and R.C. Garvie, "The Influence of Precipitate Size and Temperature on the Fracture Toughness of Calcia- and Magnesia-Partially Stabilized Zirconia", *Fract. Mech. of Ceram.*, (Ed. R.C. Bradt, A.G. Evans, D.P.H. Hasselman and F.F. Lange), 6, 339-354 (1983).
4. R.C. Garvie and M.F. Goss, "Thermal Shock Resistant Alumina/Zirconia Alloys", published in *Advanced Ceramics II*, 69-87. Ed. S. Sōmiya, Elsevier App. Sci., London, 1988.
5. R.C. Garvie, M.F. Goss, S. Marshall and C. Urbani, "Dense, Thermal Shock Resistant Advanced Refractories", *Proc. Metall. Soc. Can. Inst. Min and Metall.*, 4, "Adv. Refr. Metall. Ind.", Ed. M.A.J. Rigaud, Pergamon, New York, pp. 53-69, (1988)
6. T.M. Wehrenberg and J.R. Stein, *Glass International*, December, 19-20 (1984).
7. R.N. Enderfield, B.C. Hocking and M.G. Oxlade, "Recent Advances in Refractories for the Teeming of Steel", *Refract. J.*, Sept./Oct., 10-19, (1975).

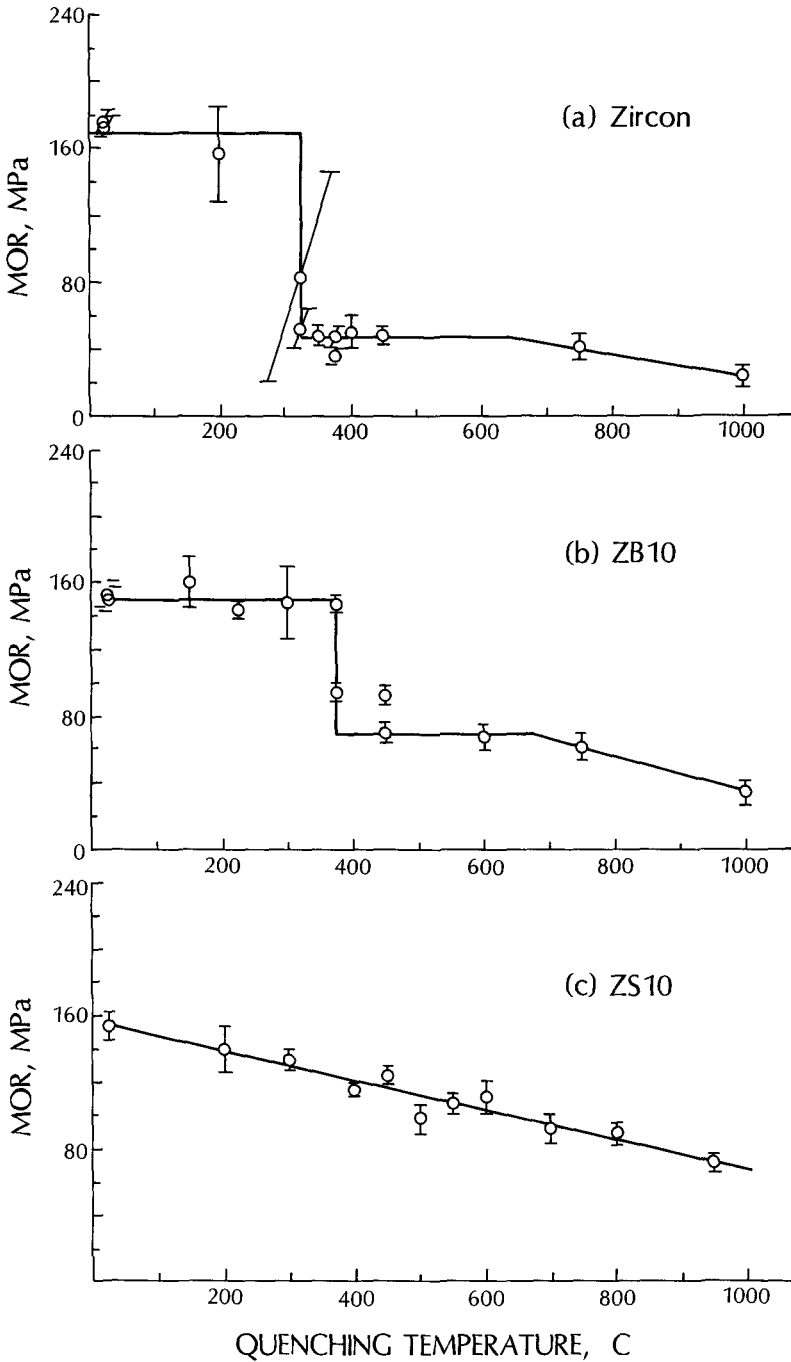
Table 1. Property Data for ZS10 and a Zircon Refractory.

<u>Property</u>	<u>Material</u>	
	<u>ZS10</u>	<u>Zircon</u>
MOR, MPa	149	21.9
Young's Modulus, MPa	188	55.6
$K_{Ic}$ , MPa m	2.9	1.5
$\tau_{WOP}$ , J/m <sup>2</sup>	73.1	20.9
$\tau_{NBT}$ , J/m <sup>2</sup>	22.2	20.8
$\tau_{WOP}/\tau_{NBT}$	3.3	1.0
Total Porosity, %	8	21

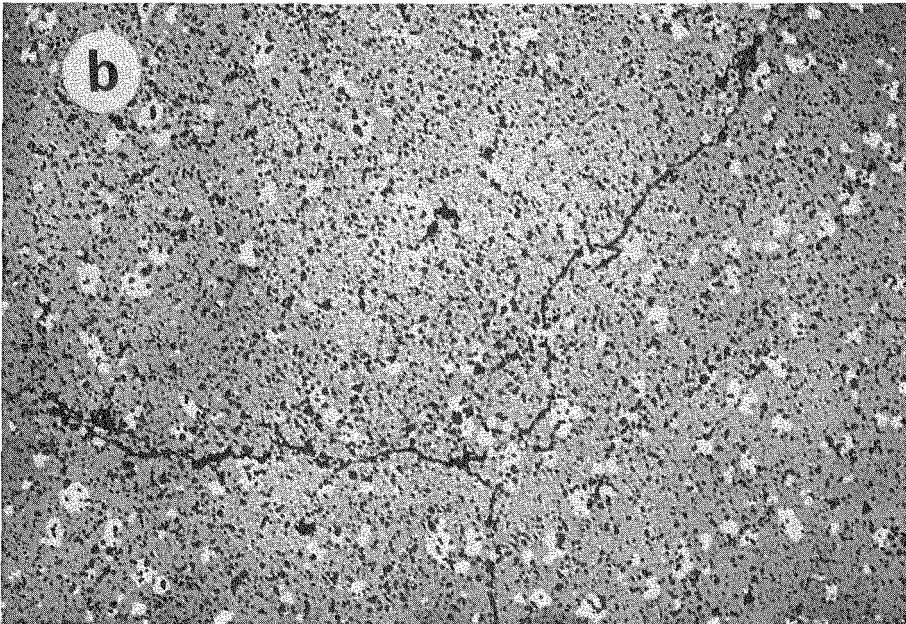
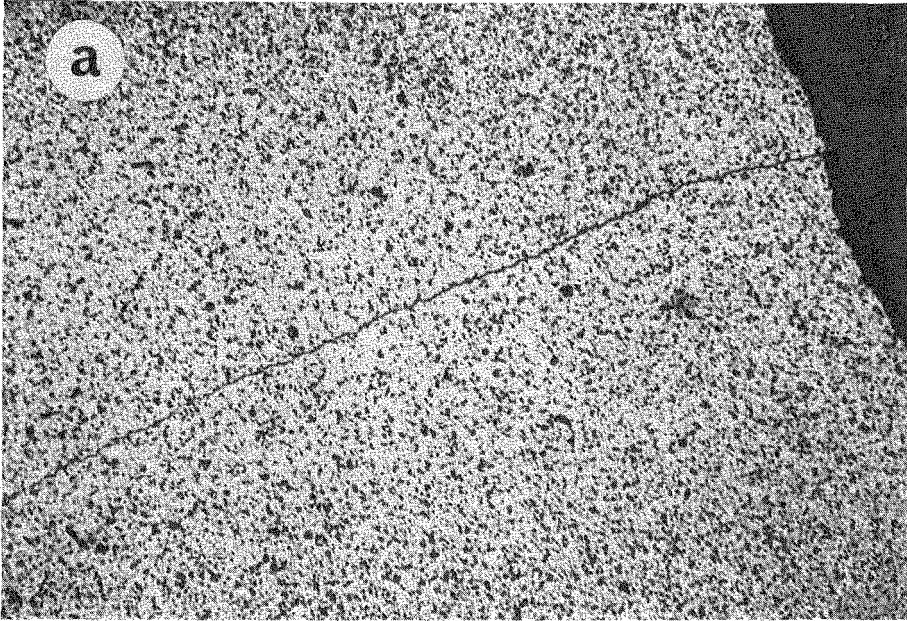
Table 2. Chemical Analysis of Zircon 20 and ZS10.

<u>Oxide</u>	<u>Amount (wt%)</u>	
	<u>Zircon 20</u>	<u>ZS10</u>
ZrO <sub>2</sub>	64.7	64.4
SiO <sub>2</sub>	34.2	32.0
Al <sub>2</sub> O <sub>3</sub>	0.25	1.7
TiO <sub>2</sub>	0.7	0.12

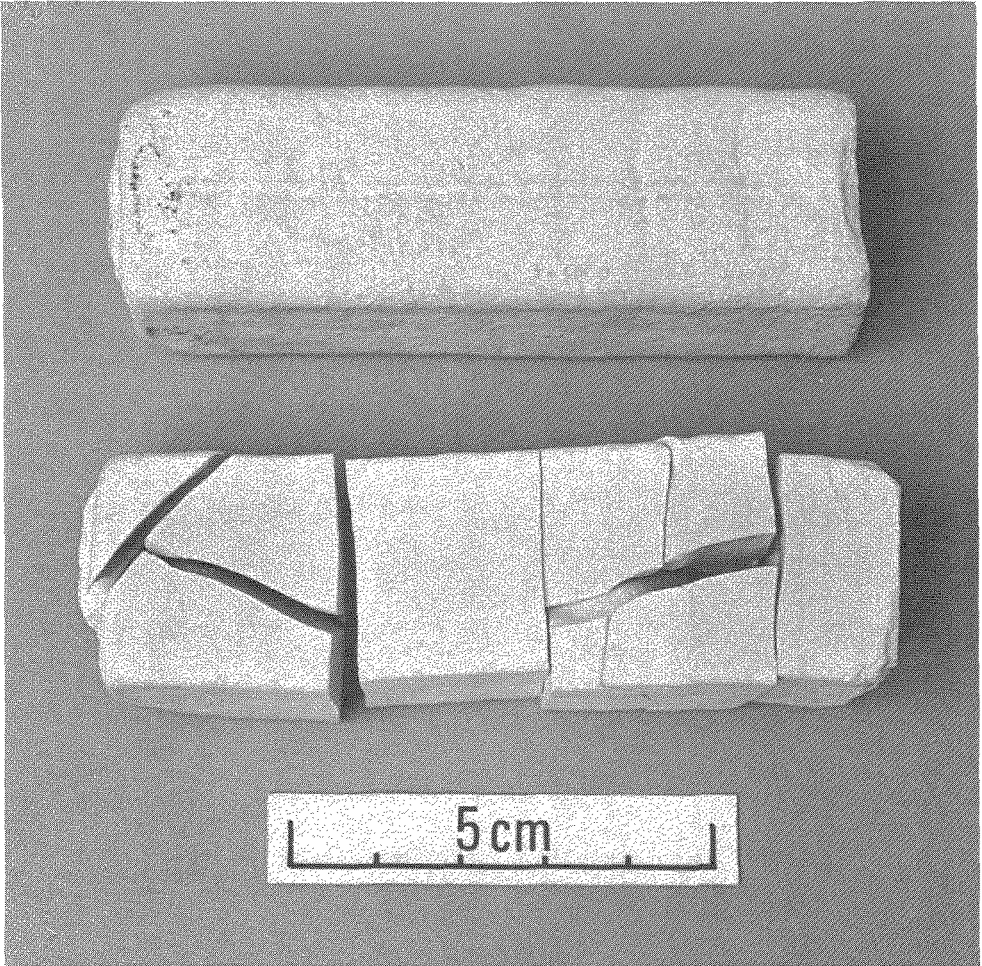




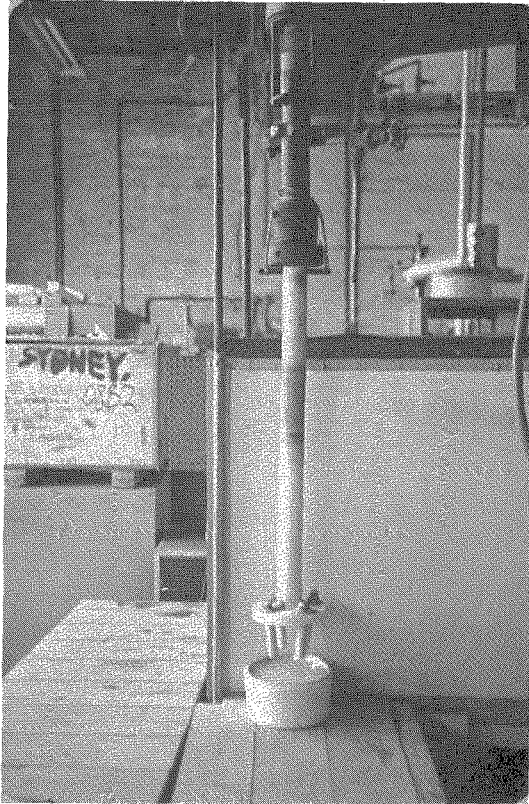
1. Thermal shock behaviour of (a) zircon, (b) the zircon/baddelyite alloy, ZB10 and (c) the zircon/MZP alloy, ZS10.



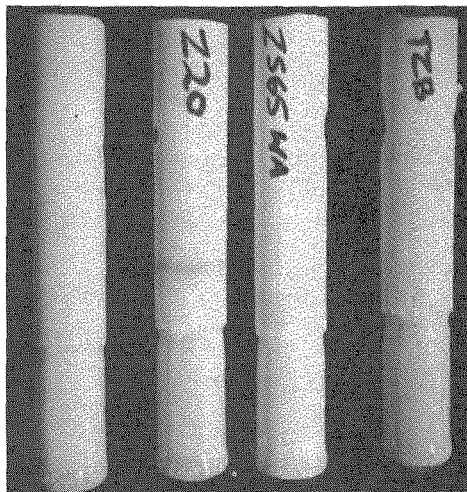
2. Optical micrographs of (a) zircon and (b) ZS10 quenched from 1000°C into water at room temperature.



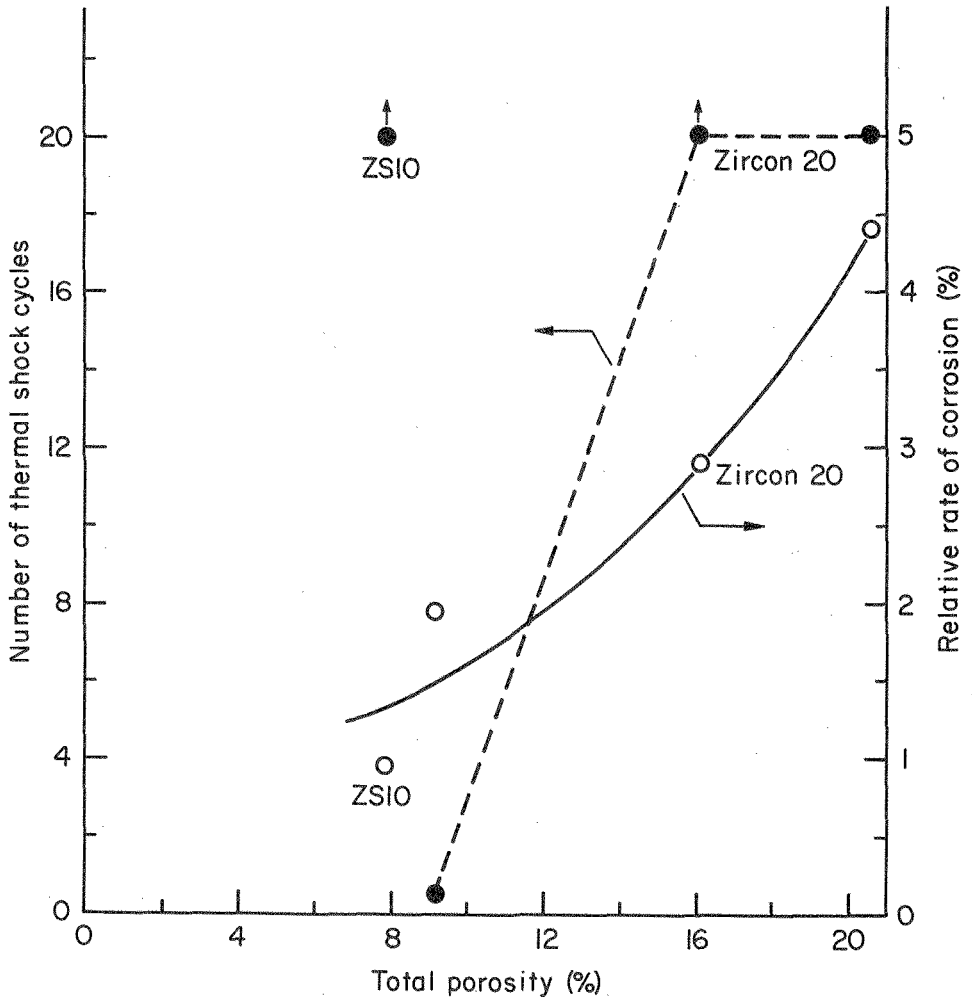
3. Photograph of ZS10 after 20 thermal fatigue cycles (top sample) and zircon after  $\frac{1}{2}$  cycle; a cycle is comprised of 1400°C/15min.-room temperature/15min.



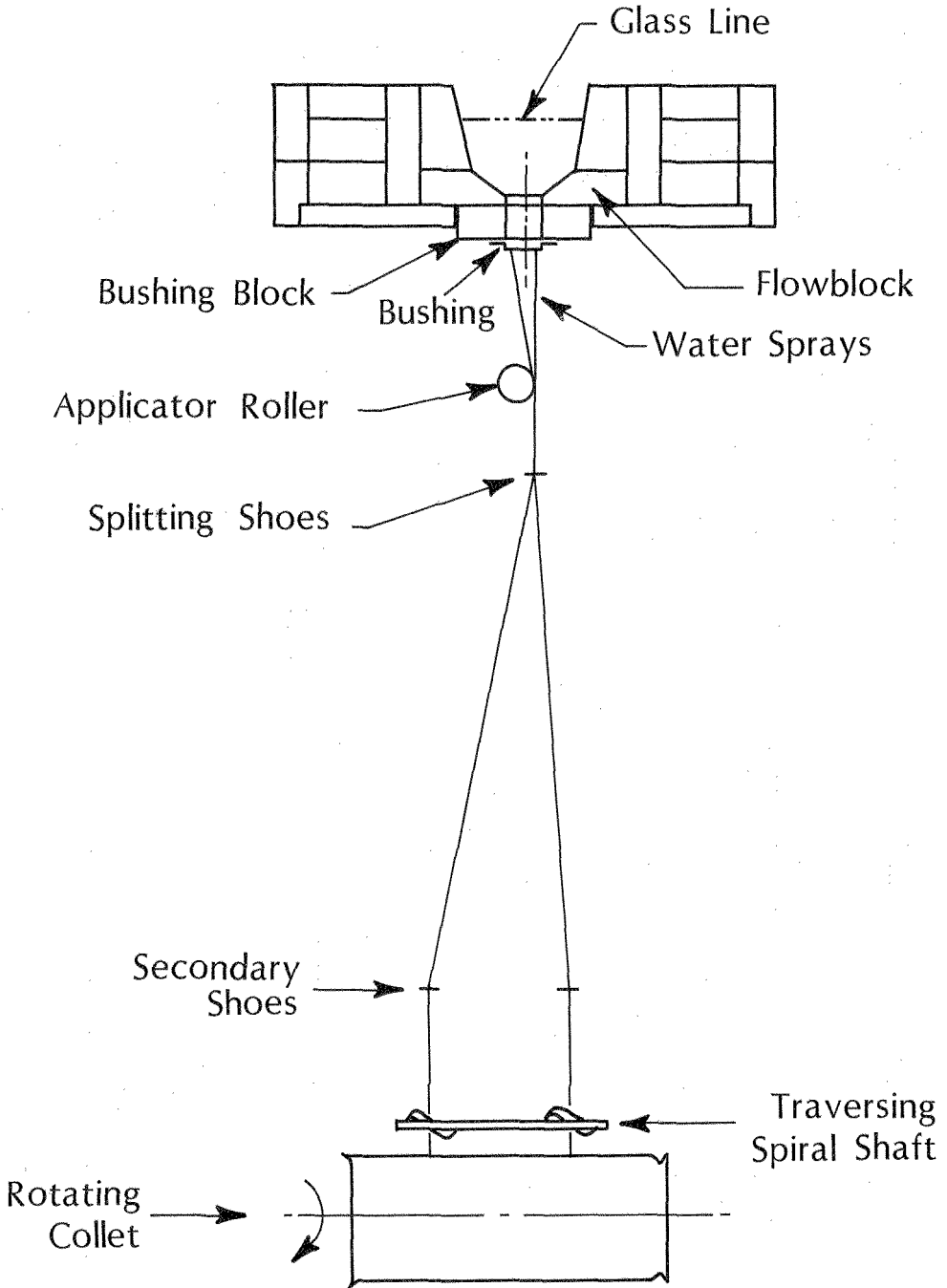
4. Photograph of test rig used to assess glass corrosion resistance of refractories at ACI Ltd.



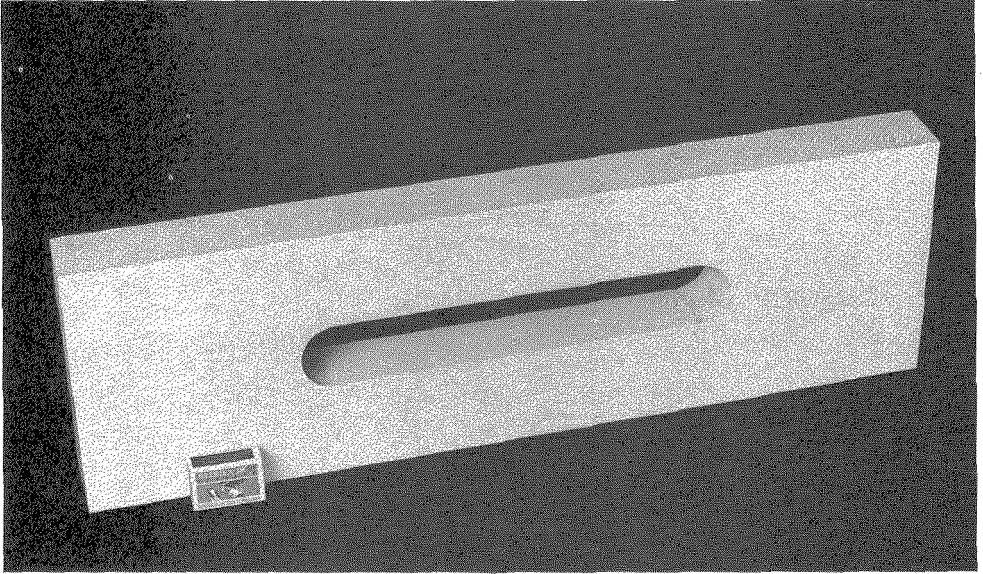
5. Photograph of ZS10 and commercial zircon refractories after testing in molten E-glass at 1330°C/235hr.



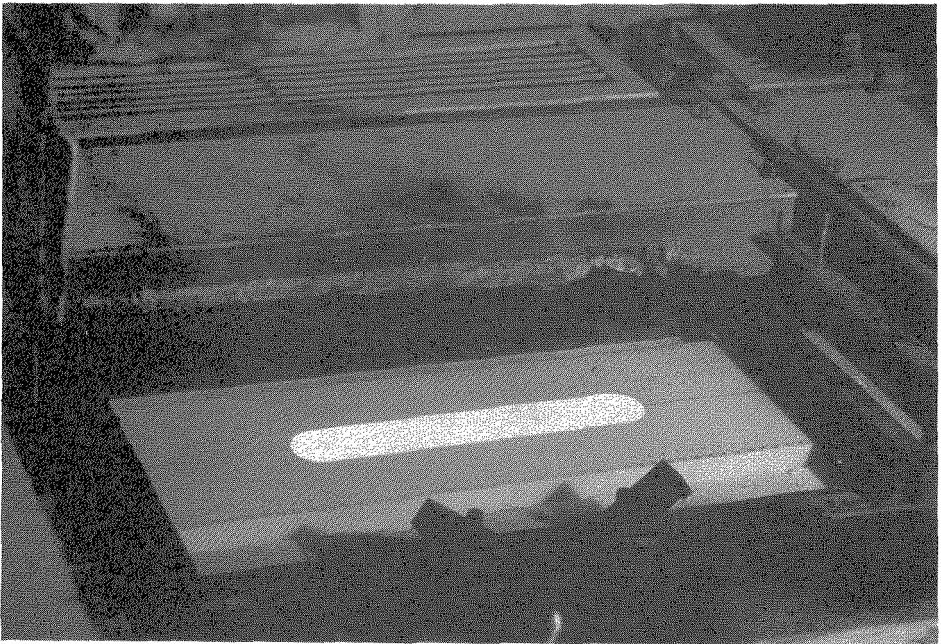
6. Porosity dependence of the thermal shock and corrosion resistance of various zircon materials.



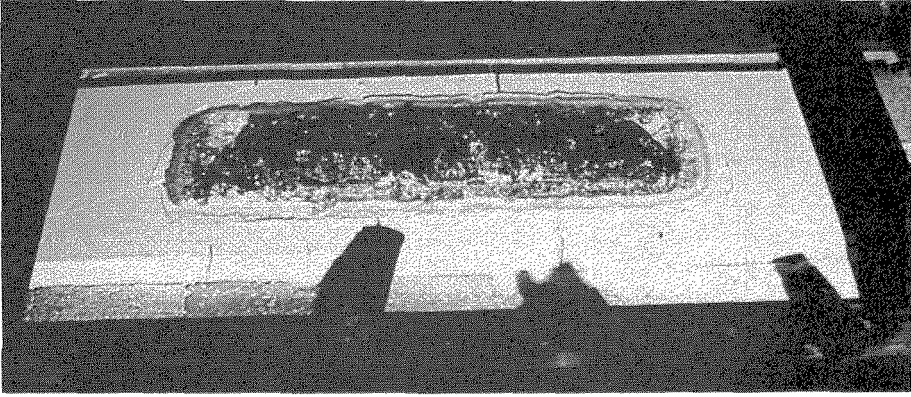
7. Schematic outline of the production process for fibreglass.



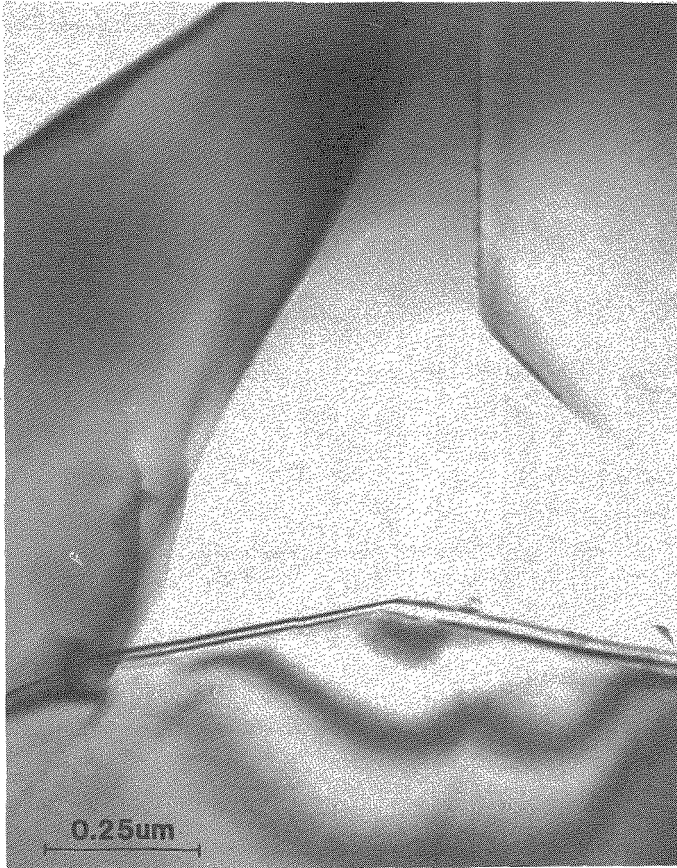
8. Photograph of a prototype bushing block made of ZS10.



9. Photograph of the ZS10 bushing block installed in position 16, number 1 tank at ACI Fibreglass.

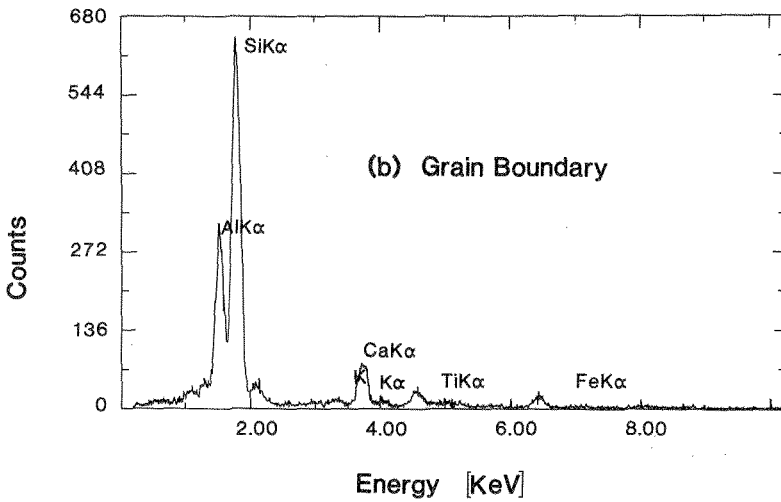
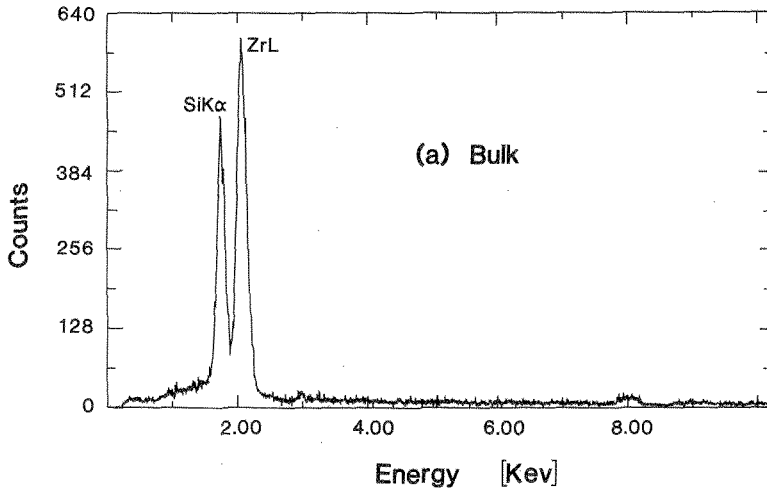


10. Photograph of the ZS10 bushing block after being in operation for 11 months and processing 386 tonnes of E-glass.

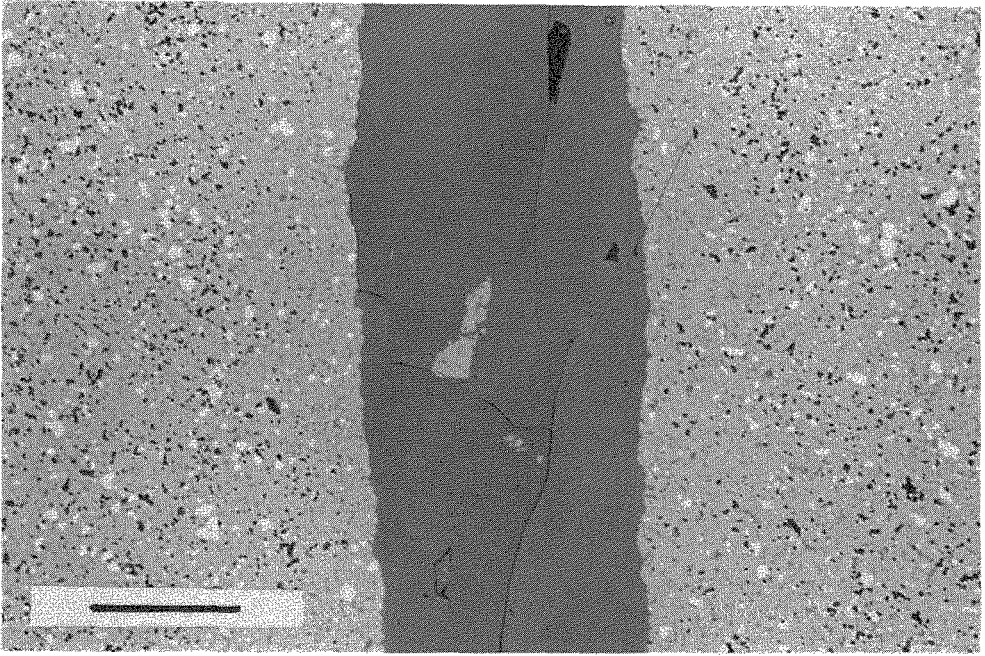


11. Bright field TEM micrograph of a triple point in a pristine sample of ZS10 showing a grain boundary glassy phase.





12. X-ray energy dispersion analyses of (a) bulk zircon and (b) a grain boundary in ZS10; the latter confirms the presence of alumina in the grain boundary.



13. Optical micrograph of the used ZS10 block showing the presence of E-glass in a crack; the glass has penetrated the bulk refractory along its grain boundaries. The bar = 50 $\mu$ m.